Alfvén Mach number and IMF clock angle dependencies of sunward flow channels in the magnetosphere

S. Eriksson[1] and L. Rastätter[2]

Received 4 February 2013; revised 26 February 2013; accepted 27 February 2013; published 11 April 2013.

[1] Interplanetary coronal mass ejections associated with strong interplanetary magnetic field (IMF) By have been shown to enhance the neutral density in low Earth orbit. The enhancement has been linked to strong downward Poynting fluxes embedded within ionospheric channels of significant sunward **E**x**B** drift (2000–3000 m/s). Here we present MHD results describing the magnetospheric counterpart of the ionospheric flow channel that Defense Meteorological Satellite Program (DMSP) encountered on 15 May 2005. It is shown that the clock angle of maximum sunward flow (θ_{FC}) depends on the IMF clock angle $\theta_{FC} = \alpha * \theta_{IMF} - 1.3°$ with α = (0.30, 0.38, 0.43, 0.45) at X = (4, 2, 0, −2) R_E. This is poleward of the magnetic null point region. The flow also depends on the solar wind Alfvén Mach number $Vx = Vx0 - \delta v * M_A$. The critical $M_A = Vx0 / \delta V$ for Vx = 0 decreases from M_A = 3.42 (X = 4 R_E) to M_A = 2.40 (X = −2 R_E). The low M_A and θ_{IMF} conditions that characterized the X = 2 R_E flow and resulted in strong Poynting flux occurred for 16% of all 167 h in 1998–2008 with *Dst* < −180 nT. **Citation:** Eriksson, S., and L. Rastätter (2013), Alfvén Mach number and IMF clock angle dependencies of sunward flow channels in the magnetosphere, *Geophys. Res. Lett.*, *40*, 1257–1262, doi:10.1002/grl.50307.

1. Introduction

[2] Field-aligned currents (FACs) are important for the coupling of energy and particle precipitation from the solar wind and magnetosphere to the ionosphere. *Anderson et al*. [2008] employed Iridium magnetometer data to generate stable Northern Hemisphere (NH) FAC maps for all directions of the interplanetary magnetic field (IMF). The FAC maps demonstrate that the most high-latitude pair of opposite FACs rotates in a statistical sense with the IMF By/Bz clock angle for northward and neutral IMF Bz. *Anderson et al*. [2008] inferred a corresponding **E**x**B** flow between the oppositely directed FACs. The proposed flow is azimuthally directed toward the northern dusk (dawn) for negative (positive) IMF By with opposite flow directions expected in the Southern Hemisphere (SH) for the same IMF By. This is known as the Svalgaard-Mansurov effect [*Svalgaard*, 1968; *Mansurov*, 1969] which is believed to be caused by IMF By-dependent flank magnetopause reconnection [e.g., *Friis-Christensen et al*., 1972; *Burch et al*., 1985; *Eriksson et al*., 2005; *Li et al*., 2011].

[3] *Eriksson et al*. [2008] reported the first direct link between a dusk-to-dawn migration of a sunward **E**x**B** flow channel across the NH polar cap and an IMF clock angle rotation from IMF By > 0 to By < 0 for an interplanetary coronal mass ejection (ICME) [*Gosling*, 1990] on 15 May 2005. A distinct pair of oppositely directed FACs was present at the migrating flow channel as observed by Defense Meteorological Satellite Program (DMSP) F13 and F15 which is consistent with the electrodynamic scenario envisioned by *Southwood* [1987] and the inferred **E**x**B** flow proposed by *Anderson et al*. [2008]. The observed link between the flow channel in the ionosphere and the IMF clock angle is in qualitative agreement with a high-latitude reconfiguration of a reconnection region [*Luhmann et al*., 1984].

[4] The 15 May 2005 event is one of several anomalous geomagnetic storms in 2004–2005 [*Knipp et al*., 2011] that resulted in poor neutral density specifications by the Mass Spectrometer and Incoherent Scatter (MSIS) model. *Crowley et al*. [2010] used the Assimilative Mapping of Ionospheric Electrodynamics (AMIE) procedure for one of these anomalous events and verified that the high 60 mW/m^2 values of localized Joule heating were present at the foot points of the near-cusp and polar cap field lines and associated them with heretofore unmodeled neutral density enhancements in this region [*Lühr et al*., 2004]. *Knipp et al*. [2011] demonstrated that the same **E**x**B** flow channels examined by *Eriksson et al*. [2008] were related to unprecedented and large earthward-directed Poynting fluxes at 850 km altitude. *Li et al*. [2011] simulated three of the anomalous events using the OpenGGCM MHD model and confirmed a direct connection between the observed localized Poynting flux enhancements and simulated intense Joule heating rates on the dayside between a pair of oppositely directed FACs. All dayside Joule heating regions mapped to a flank magnetopause reconnection region for the predominant IMF By conditions.

[5] Here we present the existence of a localized channel of sunward **E**x**B** flow on the earthward side of the NH magnetopause on the basis of a global BATSRUS MHD simulation [*Powell et al*., 1999; *Ridley et al*., 2002] performed at the NASA Community Coordinated Modeling Center (GEM_PFlux_081910_1 and GEM_PFlux_081910_1a) for the 15 May 2005 ICME. We show that the location of the simulated sunward flow channel has a linear dependence on the IMF clock angle (θ_{IMF}) and that the maximum flow within this channel has an inverse dependence on the upstream solar wind Alfvén Mach number.

[1]Laboratory for Atmospheric and Space Physics, University of Colorado, Boulder, Colorado, USA.
[2]NASA Goddard Space Flight Center, Greenbelt, Maryland, USA.

Corresponding author: S. Eriksson, Laboratory for Atmospheric and Space Physics, University of Colorado, Boulder, CO, USA. (eriksson@lasp.colorado.edu)

0094-8276/13/10.1002/grl.50307

2. MHD Simulation Results of a Magnetospheric Sunward Flow Channel

[6] Figure 1 shows the MHD simulation results of the Vx flow component in the GSM YZ plane at X = 2 R_E for four times on 15 May 2005 that correspond to some of the times of maximum observed ionospheric sunward flow by DMSP F13 and F15 [*Eriksson et al.*, 2008] during the ICME flux rope. A well-defined channel of sunward flow is present just earthward of the NH magnetopause. This channel rotates from high latitudes at dusk to low latitudes at dawn as θ_{IMF} rotates from 48° to −114°. A corresponding SH flow channel exists on the opposite side of local noon as compared with the NH channel.

[7] Figure 1 (right) shows the magnetic field topology maps [*Rastätter et al.*, 2012] centered on the NH sunward flow

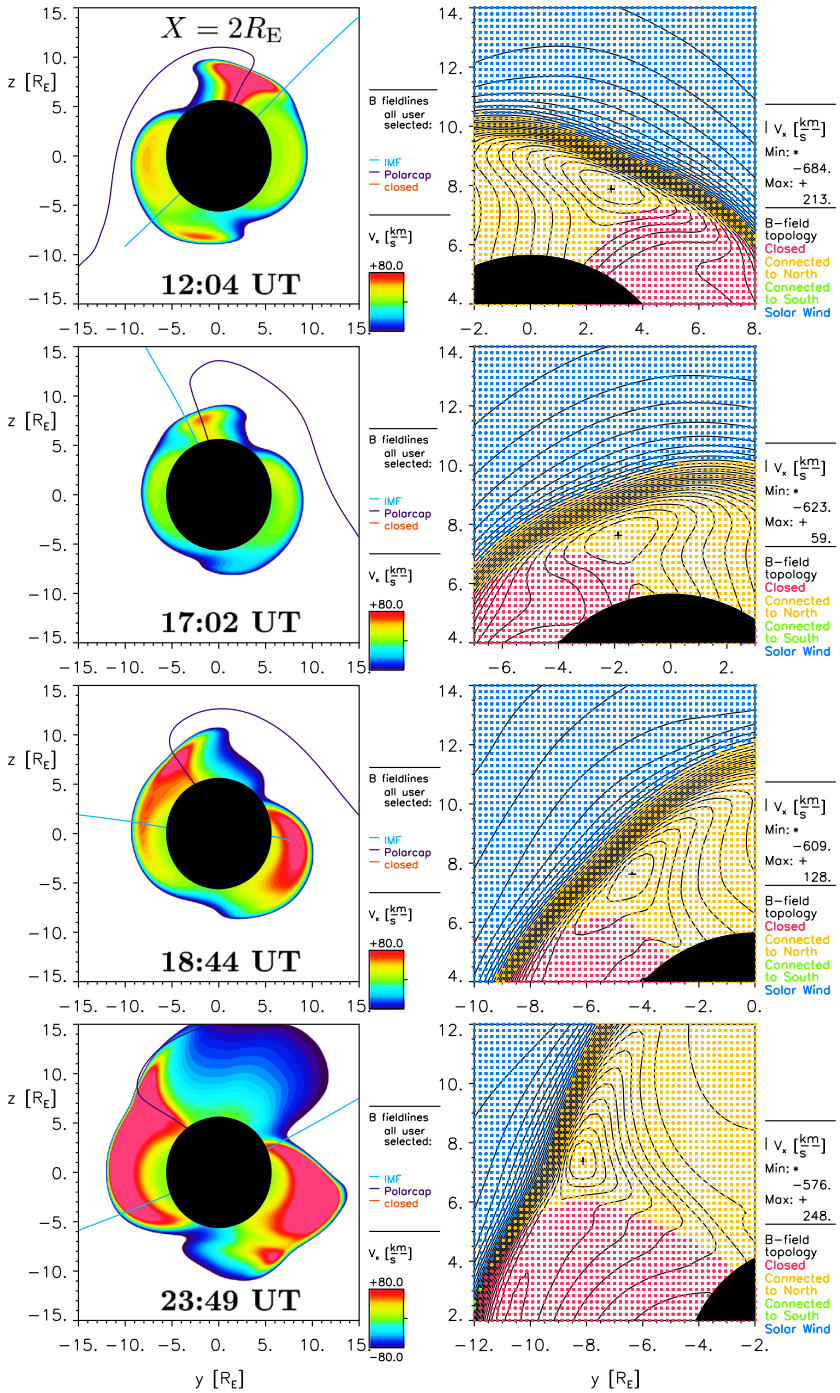

Figure 1. GSM X = 2.0 R_E plane cuts for (top to bottom) 1204, 1702, 1844, and 2349 UT on 15 May 2005. The left column shows the Vx flow component (red: sunward Vx > 0) with one IMF field line (blue) through (X, Y, Z) = (15, 0, 0) R_E and one open field line (black) passing through the X = 2.0 R_E plane of maximum Vx > 0 within the sunward flow channel. The right column shows contour plots of Vx and the magnetic field topology in blue (solar wind), red (closed magnetospheric field) and yellow (open fields connected to the Northern Hemisphere) colors.

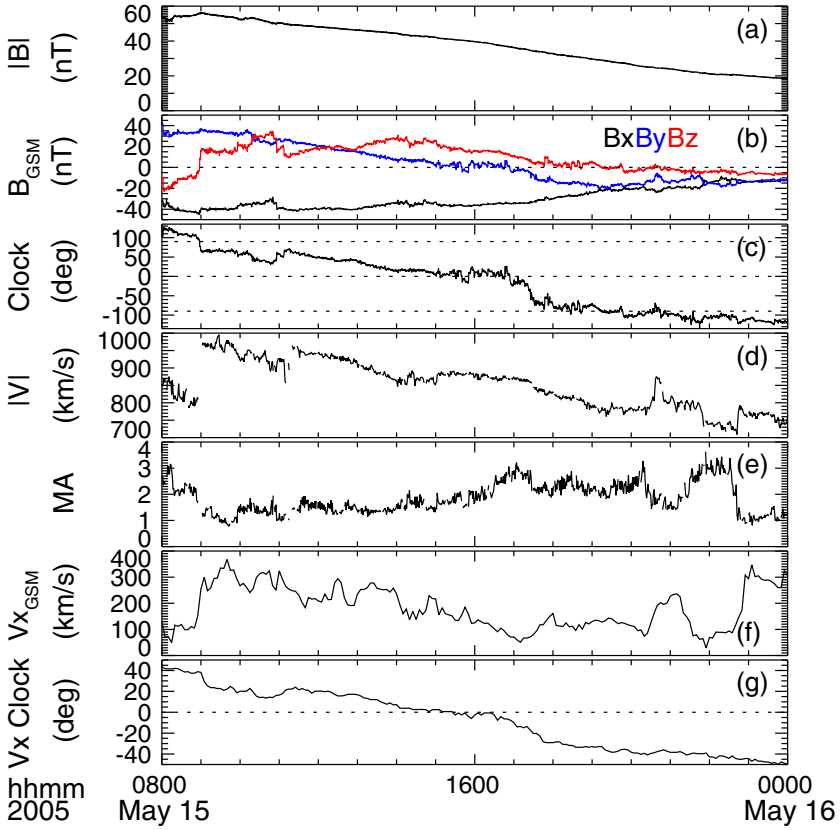

Figure 2. ACE satellite observations 08–24 UT on 15 May 2005 compared with MHD simulated sunward flow channel information. The ACE data were shifted forward in time by 32 min. The panels correspond to (a) IMF magnitude; (b) GSM magnetic field components; (c) IMF clock angle θ_{IMF} = atan(By / Bz); (d) solar wind speed; (e) Alfvén Mach number in the solar wind; (f) maximum sunward speed within the MHD simulated flow channel at X = 2 R_E; and (g) clock angle of the center location of the sunward flow channel θ_{FC} = atan(Y / Z).

channel at X = 2 R_E. The superposed flow contours show that the channel exists on open fields connected to the north (yellow) and adjacent to a closed field line region (red). Locations of maximum sunward flow within this channel are found at the plus symbol. The open geomagnetic field lines shown in Figure 1 (left) are connected to these flow maxima. They are dragged from dawn to dusk by a Vy > 0 flow within the simulated magnetospheric flow channel for IMF By < 0 which is consistent with the Svalgaard-Mansurov effect.

[8] We followed the temporal evolution of the simulated sunward flow channel on 15 May at a 5 min cadence with special emphasis on the maximum Vx flow speed and its Y and Z GSM position in the X = 2 R_E plane. The (Y, Z) coordinates were used to derive a corresponding clock angle defined as θ_{FC} = atan(Y / Z) such that a flow channel at Y = 0 and Z > 0 R_E corresponds to $\theta_{FC} = 0°$ and a dawnside (duskside) flow channel at Y < 0 (Y > 0) corresponds to $\theta_{FC} < 0°$ ($\theta_{FC} > 0°$). Figure 2 presents the resulting time series of maximum Vx (Figure 2f) and θ_{FC} (Figure 2g) during 08–24 UT and the observed IMF, solar wind speed, and solar wind Alfvén Mach number $M_A = V / V_A$ from the ACE satellite where $V_A = B / \sqrt{(\mu_0 m_p N)}$ is the Alfvén speed based on the total magnetic field magnitude and the proton number density. It is clear that θ_{FC} at X = 2 R_E is directly correlated with θ_{IMF}. There is also an apparent anti-correlation between the simulated maximum Vx speed and the observed solar wind M_A. Figure 3 illustrates these correlations in two scatter plots. A very high R = 0.99 correlation coefficient is obtained between θ_{FC} and θ_{IMF} at X = 2 R_E with a linear relation $\theta_{FC} = 0.38 * \theta_{IMF} - 1.5$. A high R = −0.91 correlation coefficient is also found between the maximum sunward speed within the flow channel just earthward of the magnetopause and the solar wind M_A observed by ACE with the functional form Vx = 421 − 129 * M_A (km/s). The M_A dependence means that the higher the Alfvén Mach number becomes in the solar wind, the slower the maximum sunward flow is within this channel at X = 2 R_E. In fact, no sunward flow is expected at X = 2 R_E for $M_A > 3.26$. This may be understood in terms of the stresses imposed on the newly reconnected field lines. The **J**x**B** force of the highly kinked open fields which forces them sunward on the sunward side of the reconnection line will not be able to accelerate these fields against the anti-sunward magnetosheath flow unless the adjacent magnetosheath is sub-Alfvénic.

[9] The magnitude and location of the sunward flow through the X = 2 R_E plane are compared with the maximum sunward flow and its clock angle position in the neighboring YZ planes X = −2, 0, 4 R_E. The results are shown in Figure 4. We find several important results from this exercise. First, there is no temporal delay of the maximum Vx flow between the different YZ planes. The flow increases or decreases simultaneously at all X locations as the external M_A decreases or increases. Second, the peak flow is actually negative (Vx < 0) at X = −2 R_E, while it is positive

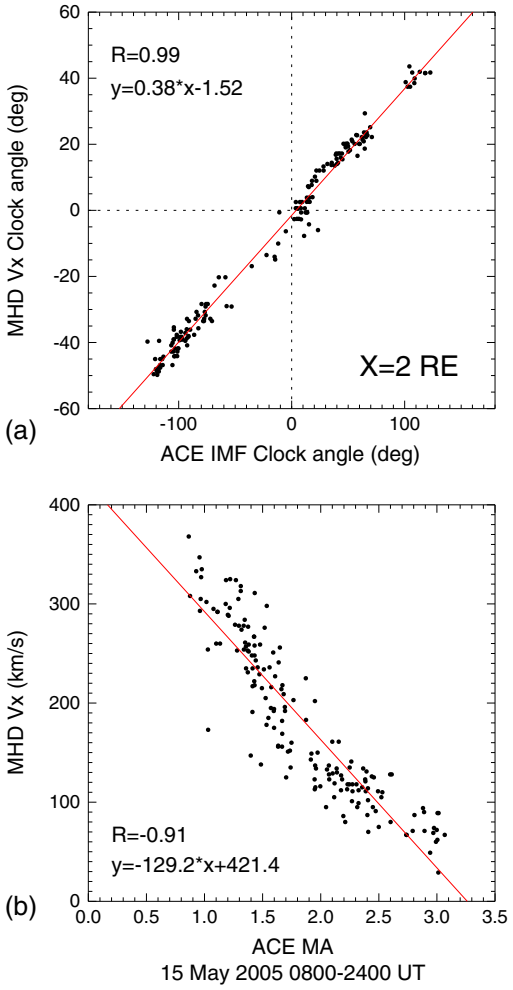

Figure 3. (a) Simulated sunward flow channel position at X = 2 R_E versus ACE IMF clock angle at 08–24 UT on 15 May 2005. (b) Simulated maximum sunward flow speed versus solar wind M_A at ACE. R is the linear correlation coefficient and y(x) is the optimum linear function shown in red lines.

(Vx > 0) at X = 2 R_E for a certain range of solar wind M_A. This suggests that the local magnetosheath M_A is super-Alfvénic adjacent to the flank magnetopause reconnection region at X = −2 R_E while it is sub-Alfvénic at X = 2 R_E such that the **J**x**B** force is unable to move the reconnected fields sunward beyond a critical downtail X location. The M_A = 1 location should slide tailward (sunward) along the magnetopause as the solar wind M_A decreases (increases). Finally, we note that the clock angle of the maximum sunward flow increases with downtail distance from X = 4 to X = −2 R_E. This is represented as $\theta_{FC} = \alpha * \theta_{IMF} + \gamma$ with different α = (0.30, 0.38, 0.43, 0.45) and γ = (-2.1°, -1.5°, −0.8°, −0.8°) at X = (4, 2, 0, −2) R_E.

[10] The M_A dependence of the maximum flow speed also varies with downtail distance as Vx = Vx0 − δV * M_A km/s where Vx0 = (301, 421, 397, 309) km/s and δV = (88, 129, 147, 129) km/s at X = (4, 2, 0, −2) R_E. The critical M_A = Vx0 / δV where the flow turns from sunward to anti-sunward within the flow channel is found to decrease with distance as M_A = (3.42, 3.26, 2.69, 2.40) at X = (4, 2, 0, −2) R_E which confirms the impact of the accelerating solar wind flow around the magnetopause and the expectation that the magnetosheath M_A = 1 boundary should slide tailward over the magnetopause as the external solar wind M_A decreases.

3. Discussion

[11] The high correlation coefficient between the location of the sunward flow channel and the IMF clock angle as well as the high correlation between the magnitude of this sunward flow and the solar wind M_A suggest that a reconnection process is involved in the generation of the magnetospheric sunward flows [e.g., *Luhmann et al*., 1984; *Li et al*., 2011]. *Siscoe et al*. [2001] presented an empirical relationship between the IMF clock angle and the clock angle of a magnetopause region of simulated minimum magnetic field strength at X = 0 R_E with x-type magnetic topology that *White et al*. [1998] referred to as the magnetospheric sash. It was found that the two angles closely followed the formula $\tan(\theta_{mp}) = -(3 \pm \sqrt{(9 + 8\tan^2(\theta_{IMF}))}) / 2\tan(\theta_{IMF})$ based on a dipole-plus-uniform vacuum superposition model of null point locations in the X = 0 plane proposed by *Yeh* [1976] and *Crooker et al*. [1990]. Figure 5 compares this vacuum superposition model of null point locations with the clock angle of the center of the simulated magnetospheric sunward flow channel in the X = 0 plane for the 15 May 2005 event. The comparison suggests that the flow channel is consistently located poleward of the null point region. *Siscoe et al*. [2001] reported that the magnetic null point location was found at increasingly larger clock angles with downtail distance which is consistent with our finding of the clock angle position of the sunward flow channel.

[12] The global MHD simulation for the ICME on 15 May 2005 resulted in a magnetospheric sunward flow channel at X = 2 R_E for the observed external conditions $M_A < 3.26$ and $|\theta_{IMF}| < 125°$ with a direct relation between M_A and the flow speed magnitude. The question is how common these conditions are in the solar wind and during strong geomagnetic storms. We know from hourly distributions of M_A and θ_{IMF} during 10 years of ACE solar wind observations (4 February 1998 to 4 February 2008) that the solar wind generally falls into the range $7 < M_A < 8$ with the IMF in the ecliptic. The observed $M_A < 3.26$ for the strong geomagnetic storm event on 15 May 2005 (*Dst* = −247 nT) only occurred for 1923 h of the entire 87,673 h of ACE data or 2.2% of the time during this 10 year period. We note that the condition $|\theta_{IMF}| < 125°$ was satisfied 79% of the time when $M_A < 3.26$. The final hourly *Dst* index indicated strong geomagnetic storms (*Dst* < −70 nT) just 2.8% of the time during the same period with low $M_A < 3.26$ occurring for 18% of all 2455 h when *Dst* < −70 nT. Periods of small $M_A = (V / B) * \sqrt{(\mu_0 m_p N)}$ naturally occur for strong IMF magnetic field strengths and moderate to low solar wind density as shown in Figure 6a. Low M_A conditions were even more common during super-storms (Figure 6b) in 1998−2008 with 29% of all 167 h of *Dst* < −180 nT occurring for $M_A < 3.26$ and 16% having both $M_A < 3.26$ and $|\theta_{IMF}| < 125°$. Although super-storms are primarily driven by ICMEs with an initial predominant southward IMF Bz ($|\theta_{IMF}| > 135°$), it is clear that *Dst* can remain very strong even for $|\theta_{IMF}| < 125°$ when we expect sunward flow channels to be present. The impact of low M_A and sunward flow channels on the overall storm-time ionosphere energy

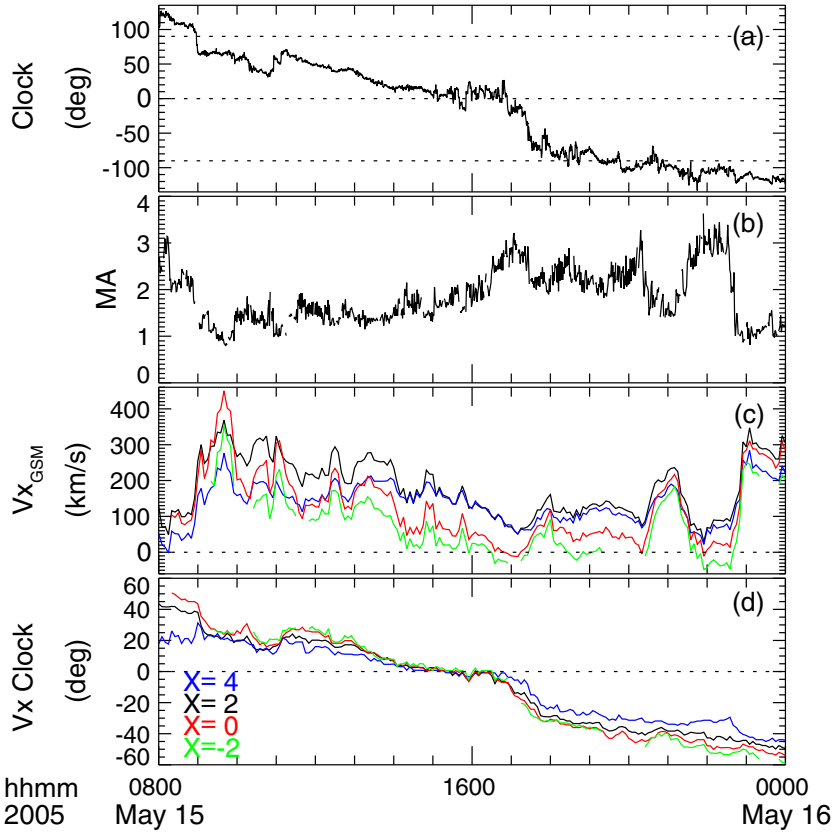

Figure 4. Time shifted (a) IMF clock angle; (b) M_A from ACE for 08–24 UT on 15 May. (c) Maximum Vx speed within MHD simulated flow channels at X = (−2, 0, 2, 4) R_E. (d) Clock angles θ_{FC} = atan(Y / Z) of the center location of the sunward flow channels in these YZ planes.

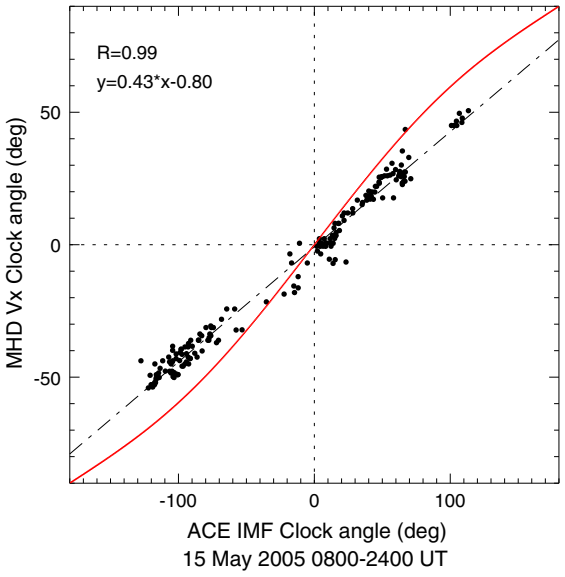

Figure 5. Clock angles of the maximum sunward flow through the X = 0 plane versus the time-shifted (32 min) IMF clock angle for the 15 May 2005 magnetic cloud at 08–24 UT (black dots). The IMF clock angle dependence of the null point locations on the magnetopause from a vacuum superposition model is shown in red.

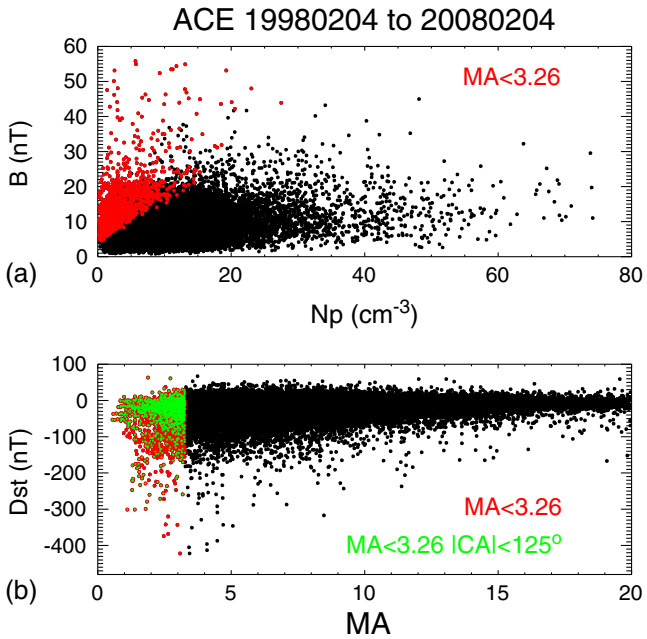

Figure 6. (a) ACE 1 h resolution magnetic field strength versus solar wind density for a 10 year period. (b) Final hourly resolution *Dst* index versus solar wind M_A. The $M_A < 3.26$ range is marked in red color in both panels, while the subset $|\theta_{IMF}| < 125°$ and $M_A < 3.26$ is marked in green color.

budget through enhanced downward Poynting flux input is unknown. Further investigations are required with specific attention on a possible relationship between the solar wind M_A and the magnitude of the downward Poynting flux and the importance of the ionospheric conductance (season, day-night, and enhanced particle precipitation) on the proposed relationship.

4. Summary

[13] The MHD simulation of the 15 May 2005 ICME has shown that a well-defined channel of sunward **E**x**B** flow existed poleward of the predicted location of magnetic reconnection from the vacuum superposition of the IMF and the geomagnetic field [*Siscoe et al*., 2001]. Its polar angle location θ_{FC} in the YZ plane is directly determined by the IMF clock angle on the form $\theta_{FC} = \alpha * \theta_{IMF} + \gamma$ with $\alpha = (0.30, 0.38, 0.43, 0.45)$ and $\gamma = (-2.1°, -1.5°, -0.8°, -0.8°)$ for $X = (4, 2, 0, -2)$ R_E where θ_{FC} and θ_{IMF} are given in degrees. The maximum sunward flow through the YZ plane at $X = (4, 2, 0, -2)$ R_E within this channel depends on the upstream solar wind Alfvén Mach number as $Vx = Vx0 - \delta V * M_A$ (km/s). The critical $M_A = Vx0 / \delta V$ where the flow is expected to turn from $Vx > 0$ to $Vx < 0$ decreases with distance downtail as $M_A = (3.42, 3.26, 2.69, 2.40)$. This is a direct result of the sunward **J**x**B** force acting on newly reconnected fields [e.g., *Eriksson et al*., 2005; *Li et al*., 2011] whether occurring at the flank magnetopause or in the high-latitude region on open lobe fields. The solar wind conditions $M_A < 3.26$ and $|\theta_{IMF}| < 125°$ that characterized the $X = 2$ R_E flow channel for the 15 May 2005 ICME and resulted in high levels (>100 mW/m^2) of downward Poynting flux occurred for 16% of all 167 h in 1998–2008 with $Dst < -180$ nT. It remains to be seen whether the magnitude of the corresponding ionospheric **E**x**B** drift within sunward flow channels and the embedded Poynting flux directly correlates with M_A in the solar wind. It is likely that sunward flow channels and enhanced Poynting fluxes exist in the ionosphere during these low M_A solar wind conditions which is potentially very important for neutral density enhancements in low Earth orbit and the resulting increased satellite drag [*Lühr et al*., 2004; *Crowley et al*., 2010].

[14] **Acknowledgments.** S.E. acknowledges support by NSF grant AGS-1144154.

References

Anderson, B. J., H. Korth, C. L. Waters, D. L. Green, and P. Stauning (2008), Statistical Birkeland current distributions from magnetic field observations by the Iridium constellation, *Annales Geophys.*, *26*, 671.

Burch, J. L., et al. (1985), IMF By-dependent plasma flow and Birkeland currents in the dayside magnetosphere: 1. Dynamics Explorer observations, *J. Geophys. Res.*, *90*, 1577.

Crooker, N. U., G. L. Siscoe, and F. R. Toffoletto (1990), A tangent subsolar merging line, *J. Geophys. Res.*, *95*, 3787.

Crowley, G., D. J. Knipp, K. A. Drake, J. Lei, E. Sutton, and H. Lühr (2010), Thermospheric density enhancements in the dayside cusp region during strong By conditions, *Geophys. Res. Lett.*, *37*, L07110, doi:10.1029/2009GL042143.

Eriksson, S., et al. (2005), On the generation of enhanced sunward convection and transpolar aurora in the high-latitude ionosphere by magnetic merging, *J. Geophys. Res.*, *110*, A11218, doi:10.1029/2005JA011149.

Eriksson, S., M. R. Hairston, F. J. Rich, H. Korth, Y. Zhang, and B. J. Anderson (2008), High-latitude ionosphere convection and Birkeland current response for the 15 May 2005 magnetic storm recovery phase, *J. Geophys. Res.*, *113*, A00A08, doi:10.1029/2008JA013139.

Friis-Christensen, E., K. Lassen, J. Wilhjelm, J. M. Wilcox, W. Gonzalez, and D. S. Colburn (1972), Critical component of the interplanetary magnetic field responsible for large geomagnetic effects in the polar cap, *J. Geophys. Res.*, *77*, 3371.

Gosling, J. T. (1990), Coronal mass ejections and magnetic flux ropes in interplanetary space, in *Physics of Magnetic Flux Ropes*, *Geophys. Monogr*, *vol. 58*, edited by E. R. Priest, L. C. Lee, and C. T. Russell, pp. 343–364 AGU, Washington, DC., doi:10.1029/GM058p0343.

Knipp, D., S. Eriksson, L. Kilcommons, G. Crowley, J. Lei, M. Hairston, and K. Drake (2011), Extreme Poynting flux in the dayside thermosphere: Examples and statistics, *Geophys. Res. Lett.*, *38*, L16102, doi:10.1029/2011GL048302.

Li, W., D. Knipp, J. Lei, and J. Raeder (2011), The relation between dayside local Poynting flux enhancement and cusp reconnection, *J. Geophys. Res.*, *116*, A08301, doi:10.1029/2011JA016566.

Luhmann, J. G., R. J. Walker, C. T. Russell, N. U. Crooker, J. R. Spreiter, and S. S. Stahara (1984), Patterns of potential magnetic field merging sites on the dayside magnetopause, *J. Geophys. Res.*, *89*, 1739.

Lühr, H., M. Rother, W. Köhler, P. Ritter, and L. Grunwaldt (2004), Thermospheric up-welling in the cusp region: Evidence from CHAMP observations, *Geophys. Res. Lett.*, *31*, L06805, doi:10.1029/2003GL019314.

Mansurov, S. M. (1969), New evidence of a relationship between magnetic fields in space and on earth, *Geomagn. Aeron.*, Engl. Transl., *9*, 622.

Powell, K. G., P. L. Roe, T. J. Linde, T. I. Gombosi, and D. L. De Zeeuw (1999), A solution adaptive upwind scheme for ideal magnetohydrodynamics, *J. Comput. Phys.*, *154*, 284.

Rastätter, L., M. M. Kuznetsova, D. G. Sibeck, and D. H. Berrios (2012), Scientific visualization to study flux transfer events at the Community Coordinated Modeling Center, *Adv. Space Res.*, *49*, 1623, doi:10.1016/j.asr.2011.12.034.

Ridley, A. J., K. C. Hansen, G. Tóth, D. L. De Zeeuw, T. I. Gombosi, and K. G. Powell (2002), University of Michigan MHD results of the Geospace Global Circulation Model metrics challenge, *J. Geophys. Res.*, *107*(A10), 1290, doi:10.1029/2001JA000253.

Siscoe, G. L., G. M. Erickson, B. U. Ö. Sonnerup, N. C. Maynard, K. D. Siebert, D. R. Weimer, and W. W. White (2001), Magnetospheric sash dependence on IMF direction, *Geophys. Res. Lett.*, *28*, 1921.

Svalgaard, L. (1968), Sector structure of the interplanetary magnetic field and daily variations of the geomagnetic field at high latitudes, *Geophys. Pap. R-6*, Dan. Meteorol. Inst., Charlottenlund, Denmark.

Southwood, D. J. (1987), The ionospheric signature of flux transfer events, *J. Geophys. Res.*, *92*, 3207.

White, W. W., G. L. Siscoe, G. M. Erickson, Z. Kaymaz, N. C. Maynard, K. D. Siebert, B. U. Ö. Sonnerup, and D. R. Weimer (1998), The magnetospheric sash and the cross-tail S, *Geophys. Res. Lett.*, *25*, 1605.

Yeh, T. (1976), Day side reconnection between a dipolar geomagnetic field and a uniform interplanetary field, *J. Geophys. Res.*, *81*, 2140.